

# Ultrafine platinum nanoparticles in zirconia nanofilms: Preparation and thermal stability

Junhui He<sup>a,b,\*</sup>, Emi Muto<sup>b</sup>, Toyoki Kunitake<sup>b,a</sup>, Shuxia Liu<sup>a</sup>, Shen Zhang<sup>a</sup>, Xiangmei Liu<sup>a</sup>

<sup>a</sup> Functional Nanomaterials Laboratory and Key Laboratory of Organic Optoelectronic Functional Materials and Molecular Engineering, Technical Institute of Physics and Chemistry, Chinese Academy of Sciences (CAS), Zhongguancun Beiyitiao 2, Haidianqu, Beijing 100080, China

<sup>b</sup> Frontier Research System, The Institute of Physical and Chemical Research (RIKEN), 2-1 Hirosawa, Wako, Saitama 351-0198, Japan

Received 8 November 2007; in final form 4 February 2008

Available online 8 February 2008

## Abstract

Ultrafine Pt nanoparticles were facily prepared in zirconia nanofilms, and possessed unexpected high thermal stability due to spatial confinement, morphological change, and lattice matching in addition to the strong bonding interaction between the surface atoms of the nanoparticle and the surrounding oxygen atoms of the ZrO<sub>2</sub> matrix.

© 2008 Elsevier B.V. All rights reserved.

## 1. Introduction

Nanoparticles of metals and semiconductors are attracting much attention, as they possess promise in photonic, electronic, magnetic, and chemical applications [1,2]. Thin films consisting of such nanoparticles are especially interesting and important as new functional materials. Nanoparticles are usually synthesized in solutions by chemical, photochemical, radiolytic and hydrothermal reactions. Thus, effective immobilization of nanoparticles within the matrix or on the surface of an ultrathin film is required in most cases of practical applications, and becomes one of the major challenges in fabrication of functional thin films [3]. Efforts have also been dedicated to in situ preparation of nanoparticles in films of micrometer and sub-micrometer thicknesses. However, in those methods, nanoparticle loadings are often low and, in addition, care must be taken to avoid aggregation and precipitation of metal salts and coalescence of metallic particles [4].

Recently we developed a new ion-exchange method for incorporation of metal ions into amorphous TiO<sub>2</sub> films [5]. A variety of metal ions can be introduced, and the amount of metal ions incorporated is readily controlled by the amount of template and ion-exchange conditions. Incorporation of two or more metal species is also possible by simultaneous or sequential procedures. Such films are nanoporous, and serve as a nanoreactor for in situ synthesis of nanoparticles, as indicated by formation of noble metal nanoparticles [6], by reversible chemical transformation between metal and oxide moieties [7], and by successful preparation of bimetallic nanoparticles in such ultrathin films [8]. It is worthy of notice that ligand-free metallic nanoparticles are stably kept in the TiO<sub>2</sub> matrix. The stability probably arises from strong bonding interaction between the surface atoms of the nanoparticle and the surrounding oxygen atoms of the TiO<sub>2</sub> matrix [8], as also demonstrated for the stabilization of a Ti metal cluster [9]. This crown ether effect was also found for other oxygen-rich matrices, such as cellulose fibers and porous ZrO<sub>2</sub> fibers [10,11]. It is expected that physicochemical properties (e.g., amorphous or crystalline) of film matrices would play an important role in the formation and stability of metal nanoparticles [12–16]. In this communication, we reported preparation of ultrafine Pt nanoparticles in zirconia nanofilms and their unexpected high thermal stability at

\* Corresponding author. Address: Functional Nanomaterials Laboratory and Key Laboratory of Organic Optoelectronic Functional Materials and Molecular Engineering, Technical Institute of Physics and Chemistry, Chinese Academy of Sciences (CAS), Zhongguancun Beiyitiao 2, Haidianqu, Beijing 100080, China. Fax: +86 10 82543535.

E-mail address: [jhhe@mail.ipc.ac.cn](mailto:jhhe@mail.ipc.ac.cn) (J. He).

elevated temperatures up to 900 °C. The mechanism of stabilization was also discussed based on structural findings revealed by high resolution electron microscopy.

## 2. Experimental

A mixture of  $\text{Mg}(\text{O-Et})_2$  (10 mM) and  $\text{Zr}(\text{O-nBu})_4$  (100 mM) in 2-ethoxyethanol was used for film assembly. Thin films were assembled layer-by-layer by immersing a substrate (e.g., cleaned quartz plate) in the precursor solution at room temperature for 3 min, followed by rinsing with toluene to remove the physisorbed species, drying with  $\text{N}_2$  and hydrolysis in air. Eight cycles of this procedure were repeated and the film thickness was estimated to be ca. 20 nm from quartz crystal microbalance (QCM) mass decrease. To remove  $\text{Mg}^{2+}$  ions, the thin film was immersed in aqueous HCl of pH 4 for 20 min, rinsed with pure water and dried with nitrogen gas. It was then treated with aqueous NaOH (pH 10) for 20 min, followed by rinsing and drying with nitrogen gas. The film on quartz plate was immersed in an aqueous solution (10 mM) of platinum (IV) chloride anhydrous ( $\text{PtCl}_4$ ) for 4 h, rinsed with pure water and dried by flushing nitrogen gas. It was then exposed to  $\text{H}_2$  plasma treatments.  $\text{H}_2$  plasma treatments were carried out on a PE-2000 Plasma Etcher (South Bay Technology, USA). The operating pressure was regulated at ca. 180 mTorr. The forward power was set at 10 W, while the reflected power was optimized [6].

Nanoparticle-containing  $\text{ZrO}_2$  nanofilm was scratched off from its quartz substrate in 2-ethoxyethanol and transferred to TEM grids ( $\text{SiO}_2$ -coated gold grid) by dispenser. The fragmented films were then observed on a JEOL JEM 2100 F/SP transmission electron microscope at 200 kV.

## 3. Results and discussion

Previous results indicated that the catalytic activity of metal nanoparticle largely depends on the ratio ( $N_S/N_T$ ) of its exposed surface atoms ( $N_S$ ) to its total atoms ( $N_T$ ) [8], and thus, the size of metal nanoparticle would play an important role in determining its catalytic activity. Rough estimation of  $N_S/N_T$  of Pt nanoparticle that has a diameter of  $d$  was carried out according to the literature [8]. The  $N_S/N_T$  value was plotted against  $d$ , and the obtained curve is shown in Fig. 1. When  $d$  is 20 nm,  $N_S/N_T$  is as low as 6.55%.  $N_S/N_T$  increases slowly to ca. 33% with decrease of  $d$  when the size of Pt nanoparticle is greater than 3.3 nm. It increases sharply, however, with decrease of  $d$  when the size of Pt nanoparticle is smaller than 3.3 nm. The reliable  $N_S/N_T$  value reaches ca. 70.4% at a diameter of 1 nm. Clearly, it would be desirable to control the size of metal nanoparticles as small as possible for catalytic purposes. Based on the above theoretical investigation, fabrication of  $\text{ZrO}_2$  nanofilms containing ultrafine Pt nanoparticles ( $\sim 1$  nm) was carried out and their thermal stability was studied.

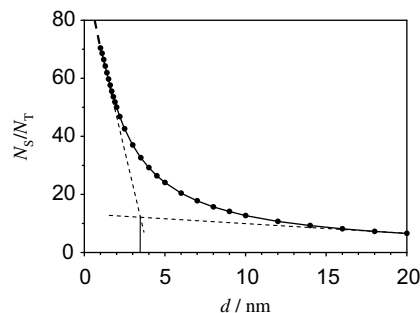


Fig. 1. Relationship between the ratio ( $N_S/N_T$ ) of exposed surface atoms ( $N_S$ ) to total atoms ( $N_T$ ) and the diameter ( $d$ ) of metal nanoparticles.

As shown in Fig. 2a, both Pt nanoparticles and  $\text{ZrO}_2$  film were clearly seen. The Pt nanoparticles are nearly spherical and distributed homogeneously in  $\text{ZrO}_2$  film. The mean diameter ( $d$ ) and its standard deviation ( $\sigma$ ) of Pt nanoparticles were estimated to be ca. 1.4 nm and ca. 0.4 nm, respectively, indicating that the particle size distribution is narrow (Fig. 2b). A selected area electron diffraction (SAED) pattern (Fig. 2c) as revealed by focusing an electron beam on the Pt nanoparticles matches that ((111), (200), (220), (311)) of cubic metallic platinum. On the other hand, when the electron beam was focused on a  $\text{ZrO}_2$  area which does not contain Pt nanoparticles, a diffuse halo appeared, indicating the amorphous nature of the as-prepared  $\text{ZrO}_2$  matrix. Fig. 2d and e shows high resolution TEM (HRTEM) images of Pt nanoparticles. A regular lattice was observed for Pt nanoparticles, and the lattice fringe reveals a periodicity of 0.22 nm, which is attributed to the (111) planes of cubic metallic platinum [17,18]. In contrast, no ordered lattice structures were observed for the  $\text{ZrO}_2$  film matrix, and the film matrix showed an amorphous, nanoporous morphology, in agreement with the SAED results.

The composition of the Pt/ $\text{ZrO}_2$  nanofilm was estimated by X-ray photoelectron spectroscopy (XPS). XPS measurements were carried out on ESCALAB 250 (VG) using Al  $K\alpha$  (1486.6 eV) radiation. The results gave the composition of the Pt/ $\text{ZrO}_2$  nanofilm as Pt:Zr = 1:2.96. Thus, high loading of platinum was realized.

The thermal stability of the Pt/ $\text{ZrO}_2$  nanofilm was investigated by annealing it at 500 °C, 700 °C, and 900 °C. The obtained specimen was observed by TEM, and the mean diameter ( $d$ ) and standard deviation ( $\sigma$ ) were determined by sampling over 100 Pt nanoparticles (histograms not shown). The effect of temperature on the particle mean diameter and standard deviation is shown both in Fig. 3 and Table 1. After annealing at 500 °C for 5 h, only the mean diameter of Pt nanoparticle increased slightly to ca. 2.0 nm from that (ca. 1.4 nm) of the as-prepared Pt nanoparticle. Additional annealing at 700 °C caused larger increases in mean diameter and standard deviation to ca. 4.0 nm and ca. 1.3 nm, respectively. Further annealing at 900 °C, however, only slightly increased the mean diameter and standard deviation to ca. 4.1 nm and ca. 1.5 nm, respectively.

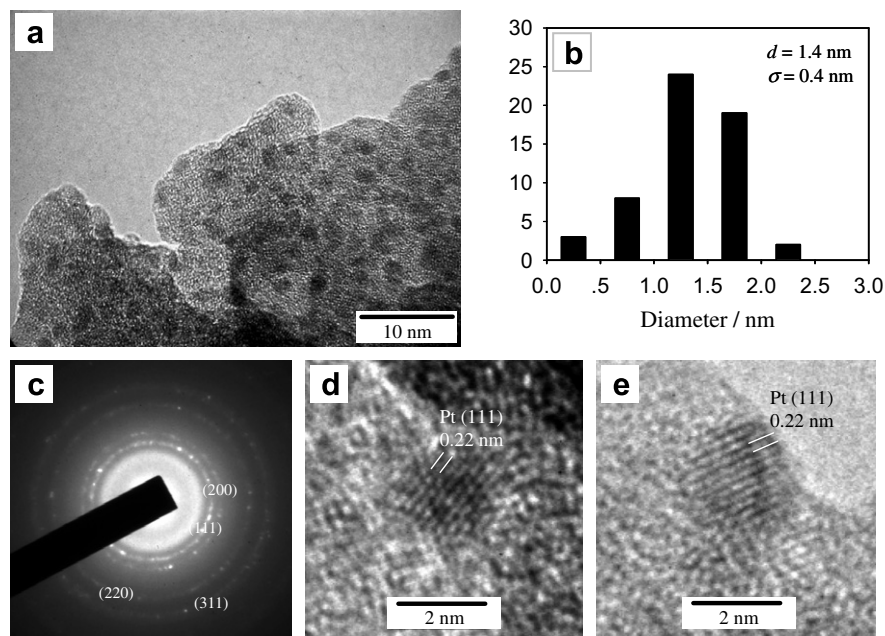


Fig. 2. TEM image (a), histogram (b), SAED pattern (c) and high resolution TEM images (d) and (e) of Pt nanoparticles in ZrO<sub>2</sub> nanofilm.

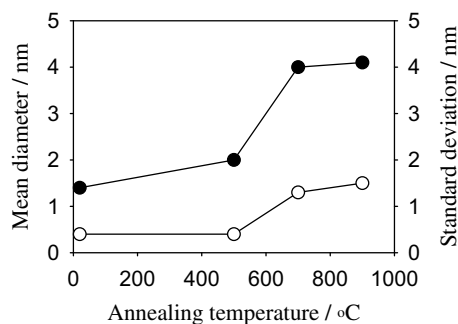


Fig. 3. Temperature dependence of particle mean diameter (●) and standard deviation (○).

Table 1  
Effect of annealing temperature on the mean diameter and standard deviation of Pt nanoparticles in ZrO<sub>2</sub> nanofilm

Annealing temperature (°C)	Mean diameter ( <i>d</i> ) (nm)	Standard deviation ( <i>σ</i> ) (nm)
As-prepared	1.4	0.4
500	2.0	0.4
700	4.0	1.3
900	4.1	1.5

HRTEM images of the as-prepared and annealed Pt/ZrO<sub>2</sub> nanofilms are compared in Fig. 4. Identical lattice fringes were observed for Pt nanoparticles, indicating the crystalline structure of Pt nanoparticle had not changed upon thermal annealing at different elevated temperatures. In contrast, unlike the as-prepared Pt/ZrO<sub>2</sub> nanofilm, after annealing at 500 °C, a regular lattice was formed in the ZrO<sub>2</sub> matrix (Fig. 4b). The majority of the lattice fringe reveals a periodicity of 0.29 nm, which is attributed to

tetragonal ZrO<sub>2</sub> [19–22]. The lattice domain size increases with increase of annealing temperature. Very interestingly, Pt nanoparticles seem to dock on ZrO<sub>2</sub> lattice domains by epitaxy, and thus the lattice of Pt nanoparticles coexists harmoniously with that of tetragonal ZrO<sub>2</sub> domains (Fig. 5). This is probably because of the small difference (0.07 nm) in the (111) spacing of Pt nanoparticles (0.22 nm) and tetragonal ZrO<sub>2</sub> domains (0.29 nm).

The unexpected high thermal stability of the Pt nanoparticles in the zirconia nanofilm would be explained in terms of spatial confinement, morphological change, and lattice matching in addition to the strong bonding interaction between the surface atoms of the nanoparticle and the surrounding oxygen atoms of the ZrO<sub>2</sub> matrix [8]. The particle transferring model is often used to account for sintering of supported metals [23]. In this model, metal microcrystals are supposed to exist in a quasi-liquid state when the temperature is beyond their Tamman temperature (0.4 times the metal melting point in Kelvin). Thus, the metal microcrystals could transfer, collide, and grow up on the surface of support over their Tamman temperature. Because of their smaller sizes, Pt nanocrystals must have an even lower Tamman temperature than Pt microcrystals (544 °C). Thus, they might still exist in their solid state and hardly grow up at below 500 °C. This speculation was supported by the negligible increase of the mean diameter and standard deviation in the temperature range of 20–500 °C. The mean diameter and standard deviation increased evidently faster in the range 500–900 °C than below 500 °C. In this range, Pt nanoparticles might be in the quasi-liquid state and began to transfer and grow. Nevertheless, the increase was surprisingly not significant, compared with in other matrices such as TiO<sub>2</sub>. The Pt nanoparticles were located within the nanopores of the

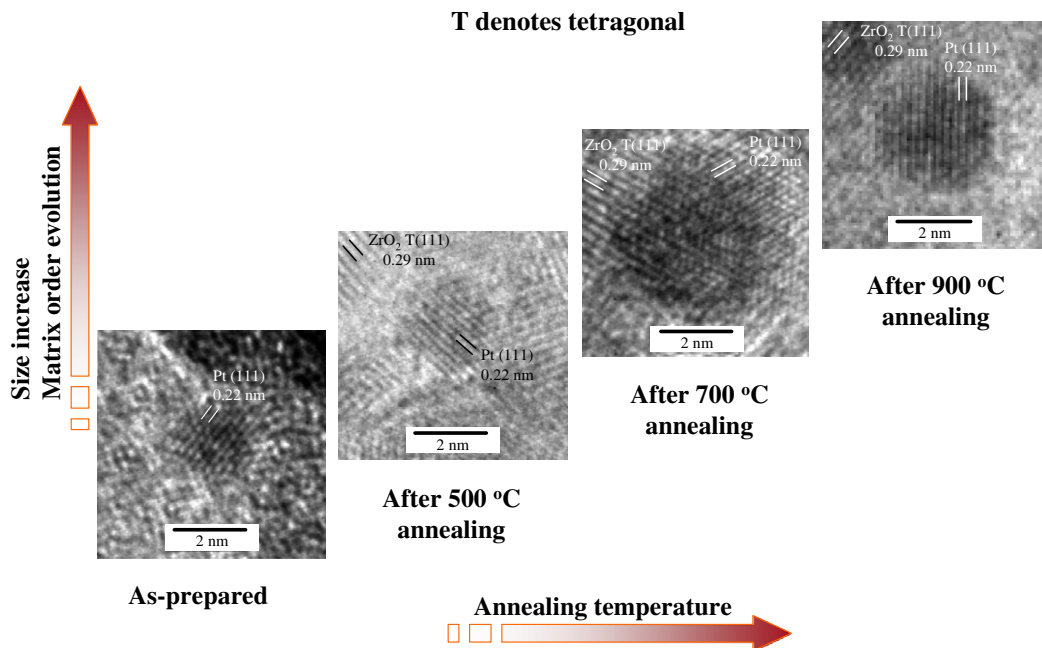


Fig. 4. HRTEM images of the Pt/ZrO<sub>2</sub> nanofilm before and after annealing at elevated temperatures.

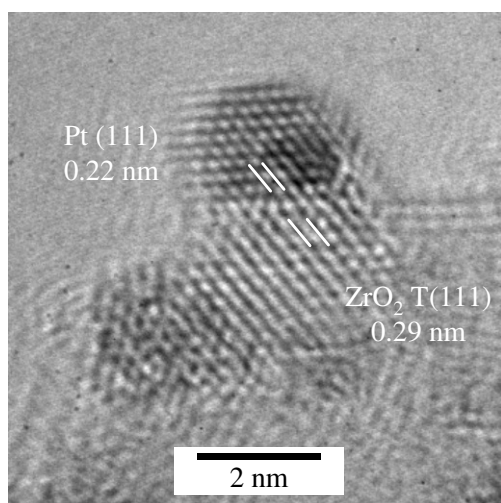


Fig. 5. HRTEM image that shows harmonious coexistence of Pt nanocrystal and tetragonal ZrO<sub>2</sub> domain by epitaxy. This image was taken after annealing at 500 °C, T denotes tetragonal.

zirconia nanofilm [5–8,11]. The confining effect of these nanopores on Pt nanoparticles may make them less easy to transfer and grow. Clearly, it is difficult for Pt nanoparticles to grow up beyond the confining nanopores of the zirconia nanofilm.

It was found previously that significant growth of three dimensional nanocrystals of matrix would largely affect the stability of imbedded metal nanoparticles, i.e., the three dimensional nanocrystals of matrix would exclude molten metal nanoparticles, causing their fusion and significant growth. One of such cases was found in titania matrices [11]. Although HRTEM revealed the appearance and expansion of tetragonal ZrO<sub>2</sub> domains at elevated temper-

atures, these tetragonal domains, unlike TiO<sub>2</sub> matrices, had not grown to three dimensional crystals [24]. Thus, they would not exclude molten Pt nanoparticles at elevated temperatures, and the fusion of molten Pt nanoparticles was suppressed.

The unveiled lattice matching of Pt nanoparticles and tetragonal ZrO<sub>2</sub> domains above should also contribute to the unexpected high thermal stability of the Pt nanoparticles in the ZrO<sub>2</sub> nanofilm. The fact that the lattice of Pt nanoparticles coexists harmoniously with that of tetragonal ZrO<sub>2</sub> domains by epitaxy suggests that the tetragonal ZrO<sub>2</sub> domains enhanced the stability of the Pt nanoparticles rather than excluded them from the ZrO<sub>2</sub> matrix. These Pt nanoparticles were, therefore, very stable in the ZrO<sub>2</sub> nanofilm.

Clearly, the zirconia nanofilm effectively immobilized and isolated Pt nanoparticles. Therefore, Pt nanoparticles in the as-prepared zirconia nanofilm had unexpected high thermal stability.

#### 4. Conclusions

In summary, the relationship between the ratio of exposed surface atoms to total atoms and the diameter of metal nanoparticles was investigated by theoretical calculations. Based on these results, we carried out and succeeded in fabrication of zirconia nanofilms containing ultrafine Pt nanoparticles. The Pt nanoparticles showed unexpected high thermal stability, which was discussed in terms of spatial confinement, morphological change, and lattice matching in addition to the strong bonding interaction between the surface atoms of the nanoparticle and the surrounding oxygen atoms of the ZrO<sub>2</sub> matrix [8]. The zirconia matrix,

however, experienced a morphological change from amorphous nature to tetragonal  $\text{ZrO}_2$  domains, and the expansion of these tetragonal domains within the matrix. Such highly stable Pt/ $\text{ZrO}_2$  composites are expected to have wide applications, especially in catalysis.

### Acknowledgments

This work was supported by Toyota Central Laboratories, the National Natural Science Foundation of China (Grant No. 20471065), and ‘Hundred Talents Program’ of CAS.

### References

- [1] G. Schmid, Chem. Rev. 92 (1992) 1709.
- [2] M.P. Pileni, in: D.L. Feldheim, C.A. Foss Jr. (Eds.), Metal Nanoparticles: Synthesis Characterization and Applications, Marcel Dekker, New York, 2001, p. 207.
- [3] J. He, T. Kunitake, in: M.P. Pileni (Ed.), Nanocrystals Forming Mesoscopic Structures, Wiley-VCH, Weinheim, 2005, p. 91.
- [4] I.-W. Shim, S. Choi, W.-T. Noh, J. Kwon, J.Y. Cho, D.Y. Chae, K.-S. Kim, Bull. Korean Chem. Soc. 22 (2001) 772.
- [5] J. He, I. Ichinose, S. Fujikawa, T. Kunitake, A. Nakao, Chem. Mater. 14 (2002) 3493.
- [6] J. He, I. Ichinose, T. Kunitake, A. Nakao, Langmuir 18 (2002) 10005.
- [7] J. He, I. Ichinose, S. Fujikawa, T. Kunitake, A. Nakao, Chem. Commun. (2002) 1910.
- [8] J. He, I. Ichinose, T. Kunitake, A. Nakao, Y. Shiraishi, N. Toshima, J. Am. Chem. Soc. 125 (2003) 11034.
- [9] R. Franke, J. Rothe, J. Pollmann, J. Hormes, H. Boennemann, W. Brijoux, Th. Hindenburg, J. Am. Chem. Soc. 118 (1996) 12090.
- [10] J. He, T. Kunitake, A. Nakao, Chem. Mater. 15 (2003) 4401.
- [11] J. He, T. Kunitake, Chem. Mater. 16 (2004) 2656.
- [12] K. Akamatsu, S. Ikeda, H. Nawafune, S. Deki, Chem. Mater. 15 (2003) 2488.
- [13] J.I. Abes, R.E. Cohen, C.A. Ross, Chem. Mater. 15 (2003) 1125.
- [14] S. Joly et al., Langmuir 16 (2000) 1354.
- [15] J. Dai, M.L. Bruening, Nano Lett. 2 (2002) 497.
- [16] S. Kidambi, J. Dai, J. Li, M.L. Bruening, J. Am. Chem. Soc. 126 (2004) 2658.
- [17] J. He, T. Kunitake, A. Nakao, Chem. Commun. (2004) 410.
- [18] JCPDS Card 88-2343.
- [19] JCPDS Card 50-1089.
- [20] A.D. Polli, T. Wagner, A. Fischer, G. Weinberg, F.C. Jentoft, R. Schlöggl, M. Rühle, Thin Solid Films 379 (2000) 122.
- [21] S. Shukla, S. Seal, J. Phys. Chem. B 108 (2004) 3395.
- [22] M. Atik, C.R. Kha, P. De Lima Neto, L.A. Avaca, M.A. Aegerter, J. Zarzycki, J. Mater. Sci. Lett. 14 (1995) 178.
- [23] R. Hughes, Deactivation of Catalysts (F. Ding, N. Yuan, Trans.), first edn., Avon Books, Beijing, 1990, p. 63.
- [24] V. Richard, S. Onoue, A. Nakao, T. Kunitake, Nat. Mater. 5 (2006) 494.